

# Voxel-Aggregated Feature Synthesis: Efficient Dense Mapping for Simulated 3D Reasoning

Owen Burns

Rizwan Qureshi

University of Central Florida

Institution1 address

ow446044@ucf.edu engr.rizwanqureshi786@gmail.com

## Abstract

We address the issue of the exploding computational requirements of recent State-of-the-art (SOTA) open set multimodal 3D mapping (dense 3D mapping) algorithms and present Voxel-Aggregated Feature Synthesis (VAFS), a novel approach to dense 3D mapping in simulation. Dense 3D mapping involves segmenting and embedding sequential RGBD frames which are then fused into 3D. This leads to redundant computation as the differences between frames are small but all are individually segmented and embedded. This makes dense 3D mapping impractical for research involving embodied agents in which the environment, and thus the mapping, must be modified with regularity. VAFS drastically reduces this computation by using the segmented point cloud computed by a simulator's physics engine and synthesizing views of each region. This reduces the number of features to embed from the number of captured RGBD frames to the number of objects in the scene, effectively allowing a "ground truth" semantic map to be computed an order of magnitude faster than traditional methods. We test the resulting representation by assessing the IoU scores of semantic queries for different objects in the simulated scene, and find that VAFS exceeds the accuracy and speed of prior dense 3D mapping techniques.

## 1. Introduction

Rapid advancements in transformer [38] based models have brought us closer to realizing the long standing goal of building embodied agents capable of perceiving, planning, and acting autonomously [12]. While limited success has already been achieved in some domain-specific scenarios [13], and Large Language Models have demonstrated surprising zero-shot reasoning capabilities [42], open-set 3D perception remains impractical for most such systems.

A truly autonomous system must be able to perceive both semantic and spatial environment information in a joint rep-

resentation [3], and must be able to do so efficiently [41]. Recent research building off of 2D vision language models (VLMs) has taken a sizeable step towards that goal with the creation of open-set 3D mapping methods (dense 3D mapping) which align semantic features with point clouds. The resulting clouds can serve as inputs to 3D VLMs [11] or be used as tools by LLM-based agents [9].

Approaches to dense 3D mapping typically involve segmenting and embedding a sequence of images which are then fused into a 3D representation. The large number of similar images which must be processed in this way to achieve successful 3D fusion results in a computational load which makes these approaches unsuitable for most real time systems, especially those tasked with exploring unseen environments. Even with modern GPUs, these methods of open-set multimodal 3D mapping (dense 3D mapping) can take upwards of 15 seconds per frame [15].

The computational complexity of dense 3D mapping renders it impractical in many situations it would otherwise prove valuable. In particular, research in agentic cooperation frequently takes place in simulation, where high-fidelity perception and efficient computation are crucial for enabling realistic interaction between agents and their environments. Instead, agents are typically provided with text-based observations that leave them blind to their environment, confounding the results of such studies especially when the agents are in close proximity [26][39][1].

To address these shortcomings, we propose Voxel-Aggregated Feature Synthesis (VAFS), a novel approach to efficient dense 3D mapping. Instead of embedding each frame received, we create and embed synthetic views of the different point cloud segments in isolation, and then use voxel aggregation to ensure uniform point distribution. By reducing the computation required to implement dense 3D mapping, VAFS makes this technique viable in a broader set of domains, including research which requires real time updates. In particular, we focus on simulator-based applications as such environments readily provide segmented point clouds, further increasing the efficiency gain over fusion-

based methods. Our main contributions are as follows:

- A novel method to generate synthetic views of regions of interest in a point cloud.
- A computationally efficient approach to dense 3D mapping capable of uniquely leveraging information available in simulated environments to create ground truth semantic observations for agentic research.

## 2. Related Works

### 2.1. Multi-Modality and Perception

Multi-modal perception has seen rapid advancement in recent years. In 2D, models such as CLIP [32] and ALIGN [16] emerged to encode text and images into a shared latent space, while segmentation models such as SAM [19] and MASKFORMER [6] emerged to perform class-agnostic image segmentation. Semantic segmentation models such as OpenSeg [7] and LSeg [20] merge those tasks, creating embeddings for objects within images, while captioning models like Blip [22] go from image to text. Another trend has been integrating image understanding into pre-existing models, with nearly all major LLM providers such as OpenAI [29] and Google [36] offering native image support and open source methods coming along not long after [2][22]. More complex tasks like motion and object tracking [23][4][17][21] and 3D scene representations [30][11] have begun to be considered as well as the frontier expands. However, the considerable cost associated with these techniques, attention's  $N^2$  runtime in particular, has motivated a number of papers to explore alternatives to representing these modalities in full or ways to isolate and ignore regions of input lacking in information [40][8].

### 2.2. Dense 3D Mapping

Dense 3D mapping algorithms<sup>1</sup> generally follow these steps:

1. Capture multi-view depth images covering the whole scene
2. Compute pixel-wise features for each depth image
3. Fuse the depth images into a 3D environment representation, using some method to combine the features of two points of the fusion operation decides to merge their associated points.

In [10], 2D semantic relevancy maps are computed and projected to 3D using the RGB-D depth data, and subsequently used to compute the volume of the relevant region. Other approaches [27][18][37][24] extract 2D pixel aligned features with off-the-shelf models and perform 3D fusion with a neural field (NeRF) [34]. NeRF-based methods typically do not create a standalone 3D representation, resulting in slower semantic queries, though Gaussian splatting

has been demonstrated to be a viable means of overcoming this limitation [31]. The most common setup, detailed in ConceptFusion [15], uses simultaneous localization and mapping (SLAM) to fuse the 2D embeddings [5][33][14]. OV3D [25] takes this a step further, using text descriptions of image segments created by vision-language models instead of image embeddings to incorporate additional context. In all such setups, large overlap is needed between input images to ensure the fusion step (whether that be direct reconstruction, SLAM [35], or a NeRF [28]) can achieve a well-aligned representation. This overlap makes pre-processing the image set prohibitively expensive, and limits the usefulness of these methods for systems requiring frequently updated mappings.

## 3. Voxel Aggregated Feature Synthesis

### 3.1. Problem Specification

We define dense 3D mapping algorithms to be an algorithms which take some sequence of observations  $T \in \mathcal{T}$  (typically depth images) from the environment  $\mathcal{S}$  and constructs a 3D representation of the environment  $M \in \mathcal{M}$  where each point is associated with a semantic feature relevant to that point. Concretely,

$$\begin{aligned} \mathcal{T} &= \{(v_1, v_2, \dots, v_t) | \forall v_t \in T \exists v_i \in S(t) \text{ s.t. } o_t \equiv v_i\} \\ \mathcal{M} &= \{\{\bar{p}_j, \mathbf{F}_j\} | \bar{p}_j \in \mathbb{R}^3, \bar{F}_j \in \mathbb{R}^N, 1j \in \mathcal{S}_p\} \quad (1) \\ f &: T \rightarrow M \end{aligned}$$

We take inspiration from ConceptFusion's definition of dense 3D mapping problems, but relax the requirement that  $v$  must be a depth image and that  $\mathcal{M}$  must include normals and confidence counts to arrive at the above. These constraints are unnecessary in this context because the simulator is capable of giving us a ground truth point cloud, removing the need for us to calculate camera poses or keep track of an estimate of position error. Unfortunately, this does mean adding new constraints on the simulation environment, which are detailed in 3.2.

### 3.2. Assumptions

We assume that for simulation environment  $\mathcal{S}$  with points  $\mathcal{S}_p$  and objects  $\mathcal{S}_o$  at time step  $t$ ,  $\mathcal{S}$  is capable of providing a coordinate  $p$ , color  $r$ , and object reference  $i$  for each point  $k$  in the ground truth point cloud  $\mathcal{P}$  as follows.

$$\begin{aligned} \mathcal{P} &= \{\{\bar{p}_k, \bar{r}_k, o_k\} | \bar{p}, \bar{r} \in \mathbb{R}^3, k \in \mathcal{S}_p, o \in \mathcal{S}_o\} \\ f_p &: (\mathcal{S}, t, k) \rightarrow \{\bar{p}_k, \bar{r}_k, i_k\} \quad (2) \end{aligned}$$

We also assume that:

- All points in a given object have the same semantic meaning in the context of what information is being encoded in the pixels.

<sup>1</sup>Rigidly defined in 3.1

- The information encoded in a pixel is dependent only upon the object of which that pixel is a part.
- We have a model that can transform a view into its corresponding 2D feature defined as  $f_e : v^m \rightarrow e^m, m \in \{G, o\}$ .

In our specific implementation, we use the Mujoco simulator following after RoCo [26], and define cameras in the simulator’s XML file to follow each object in the environment at a fixed distance and angle.

### 3.3. Algorithm

**Simulation query:** At each time step  $t$ , we query the environment for current point cloud  $\mathcal{P}_t$ .

$$\mathcal{P}_t = \{f_p(\mathcal{S}, t, k) | k \in \mathcal{S}_p\} \quad (3)$$

**View Synthesis:** We then group the points by their object reference, and render a synthetic view  $v^o$  of the object corresponding to those points by aligning a camera with the average estimated normal of the points. We repeat the process for the entire set of points to get the global view  $v^G$ . This process is detailed in Algorithm 1.

---

#### Algorithm 1 View Synthesis

---

```

 $\mathcal{O} \leftarrow \{\bar{p}_k, \bar{r}_k | f_p(\mathcal{S}, t, k)[2] = o, \bar{p}_k \text{ is not an outlier}\}$ 
 $\mathcal{N} \leftarrow \text{GET\_NORMALS}(\mathcal{O})$ 
 $\mathcal{N} \leftarrow \frac{1}{|\mathcal{N}|} \sum_{n \in \mathcal{N}} n$ 
 $\mathcal{N} \leftarrow \frac{\mathcal{N}}{\|\mathcal{N}\|}$ 
 $\text{elevation} \leftarrow \arcsin(\mathcal{N}_z)$ 
 $\text{azimuth} \leftarrow \arctan\left(\frac{\mathcal{N}_y}{\mathcal{N}_x}\right)$ 
 $\mathcal{V} \leftarrow \text{RENDER}(\mathcal{O}, \text{elevation}, \text{azimuth})$ 
return  $\mathcal{V}$ 

```

---

**Local feature computation:** We then compute the set of 2D object features  $\mathcal{E}_t$  and the the 2D global feature  $e^G_t$ .

$$\begin{aligned} \mathcal{E}_t &= \{f_e(v^o) | v^o \in \mathcal{T}_t\} \\ e^G_t &= f_e(v^G) \end{aligned} \quad (4)$$

In order to contextualize the object features, we follow the method of ConceptFusion [15] to compute the importance of an object to the scene by assessing its difference from the global feature. We then use this to compute a weighted sum aggregating information from that object feature and the global feature and normalize it to get the point cloud feature  $c^o_t$ . Then, we assign these features to their corresponding points in  $\mathcal{P}_t$  to get the update concept cloud as follows:

$$\mathcal{M}^u_t = \{\{\bar{p}, c^o_t\} | \bar{p} \in \mathcal{P}_t, o \in \mathcal{P}_t \Rightarrow c^o_t \triangleq o\} \quad (5)$$

**Voxel aggregation:** We use voxel pooling to both maintain a consistent density of points in our concept cloud and

ensure that relative positioning relationships at the borders between objects are represented explicitly. Using  $\nu$  as the voxel size and  $\epsilon$  as the increment (all outcomes in 4 used 0.1 for the starting size and increment), we create a voxel grid  $\mathcal{V}$  starting from the origin and for each voxel  $\mathcal{V}_{ijk}$  add and normalize the features of all the points within to create the combined feature and take their centroid to be the new position.

$$\begin{aligned} \mathcal{V}_{ijk} &= \{\mathcal{M}^u_{ti} | \lfloor \frac{\mathcal{M}^u_{ti}}{\nu} \rfloor = (i, j, k)\} \\ \rho &\leftarrow \frac{1}{|\mathcal{V}_{ijk}|} \sum_{x \in \mathcal{V}_{ijk}} x_p \\ \phi &\leftarrow \left\| \sum_{x \in \mathcal{V}_{ijk}} x_c \right\|_2 \\ \mathcal{M}_{tijk} &\leftarrow \{\rho, \phi\} \end{aligned} \quad (6)$$

## 4. Experimental Setup and Results

One of the most common use cases for 3D dense mapping models is creating 3D semantic representations of an environment which can be queried in various modalities. To validate the performance of VAFS, We compared it to ConceptFusion [15] and LeRF [18] on the task of identifying regions in a simulated scene (we used a scene from the RoCoBench dataset [26]) that were most strongly related to the query. We found that VAFS computed the map far faster than either baseline (Table 1), while maintaining a higher IoU score across the board even on indirect semantic queries (Table 2). We also found that our synthetic view generation improved the localization abilities of VAFS compared to the fusion-based baselines. Both baselines gave additional relevance to the regions around the target region, while VAFS prevented this blurring of features (Fig. 2).

## 5. Conclusion

We present VACC as a computationally efficient way to implement dense 3D mapping algorithms in simulation, increasing the accessibility of these algorithms to simulation-based agentic research. We demonstrate an order of magnitude decrease in runtime while achieving better performance than fusion-based approaches. Future lines of work will include extending VAFS to include point cloud segmentation and testing the method on real-world footage.

## References

- [1] Michael Ahn, Anthony Brohan, Noah Brown, Yevgen Chebotar, Omar Cortes, Byron David, Chelsea Finn, Chuyuan Fu, Keerthana Gopalakrishnan, Karol Hausman, et al. Do as i can, not as i say: Grounding language in robotic affordances. *arXiv preprint arXiv:2204.01691*, 2022. 1

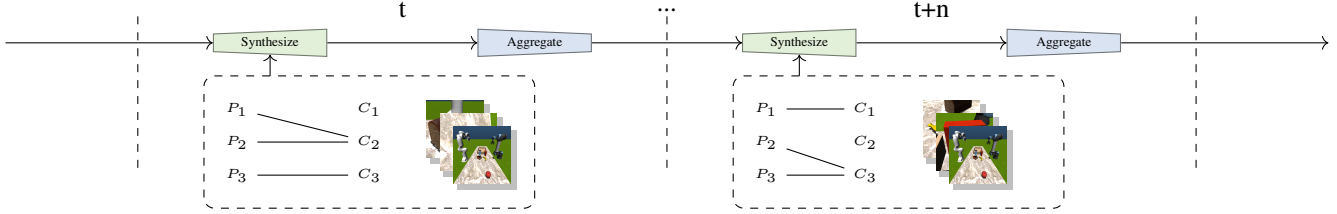


Figure 1. The high-level workflow of VAFS. At each time step, we associate points  $P$  with segments  $C$  and render views of the regions of interest. We then align embeddings of those views with the point cloud and run voxel aggregation to ensure the distribution of points remains uniform. Subsequent time steps represent updates to the point cloud, and the process runs again with new views generated for segments of the point cloud that have changed.

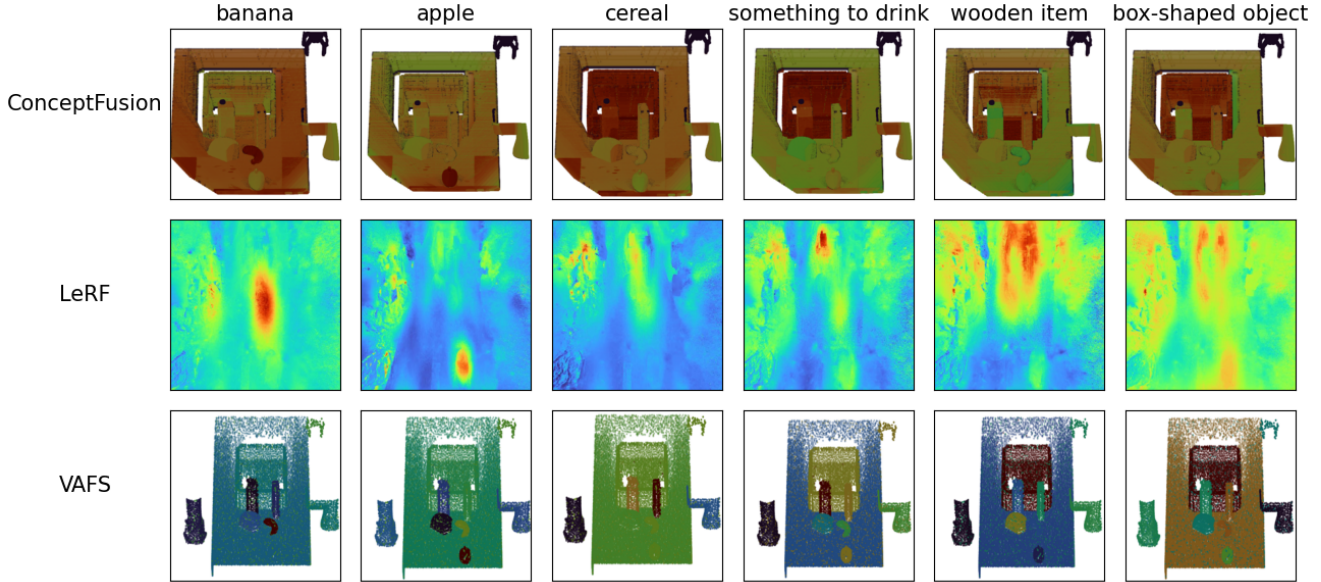


Figure 2. Relevancy maps for semantic queries.

- [2] Anas Awadalla, Irena Gao, Josh Gardner, Jack Hessel, Yusuf Hanafy, Wanrong Zhu, Kalyani Marathe, Yonatan Bitton, Samir Gadre, Shiori Sagawa, Jenia Jitsev, Simon Kornblith, Pang Wei Koh, Gabriel Ilharco, Mitchell Wortsman, and Ludwig Schmidt. Openflamingo: An open-source framework for training large autoregressive vision-language models, 2023. [2](#)
- [3] Claus-Christian Carbon. Understanding human perception by human-made illusions. *Frontiers in Human Neuroscience*, 8, 2014. [1](#)
- [4] Nicolas Carion, Francisco Massa, Gabriel Synnaeve, Nicolas Usunier, Alexander Kirillov, and Sergey Zagoruyko. End-to-end object detection with transformers, 2020. [2](#)
- [5] Boyuan Chen, F. Xia, Brian Ichter, Kanishka Rao, Keerthana Gopalakrishnan, Michael S. Ryoo, Austin Stone, and Daniel Kappler. Open-vocabulary queryable scene representations for real world planning. *2023 IEEE International Conference on Robotics and Automation (ICRA)*, pages 11509–11522, 2022. [2](#)
- [6] Bowen Cheng, Alexander G. Schwing, and Alexander Kirillov. Per-pixel classification is not all you need for semantic segmentation, 2021. [2](#)
- [7] Golnaz Ghiasi, Xiuye Gu, Yin Cui, and Tsung-Yi Lin. Scaling open-vocabulary image segmentation with image-level labels, 2022. [2](#)
- [8] Qiao Gu, Alihusein Kuwajerwala, Sacha Morin, Krishna Murthy Jatavallabhula, Bipasha Sen, Aditya Agarwal, Corban Rivera, William Paul, Kirsty Ellis, Rama Chellappa, Chuang Gan, Celso Miguel de Melo, Joshua B. Tenenbaum, Antonio Torralba, Florian Shkurti, and Liam Paull. Concept-graphs: Open-vocabulary 3d scene graphs for perception and planning, 2023. [2](#)
- [9] Qiao Gu, Alihusein Kuwajerwala, Sacha Morin, Krishna Murthy Jatavallabhula, Bipasha Sen, Aditya Agarwal, Corban Rivera, William Paul, Kirsty Ellis, Rama Chellappa, Chuang Gan, Celso Miguel de Melo, Joshua B. Tenenbaum, Antonio Torralba, Florian Shkurti, and Liam Paull. Concept-graphs: Open-vocabulary 3d scene graphs for perception and planning, 2023. [1](#)
- [10] Huy Ha and Shuran Song. Semantic abstraction: Open-

Runtime (s)			
Method	2D feature computation	3D Fusion	Total
ConceptFusion	1279	257	1536
LeRF	791	5040	5831
VACC (Ours)	<b>175</b>	<b>145</b>	<b>189</b>

Table 1. Runtime on a single Nvidia L4, processing 236 images from our simulation environment.

Text query IoU on Simulator Environment						
Method	banana	apple	cereal	something to drink	wooden item	box-shaped object
ConceptFusion	0.132	0.496	0.016	0.030	0.649	<b>0.662</b>
LeRF	0.444	0.273	0.0	0.182	0.273	0.284
VACC (Ours)	<b>0.790</b>	<b>0.656</b>	<b>0.544</b>	<b>0.733</b>	<b>0.713</b>	0.523

Table 2. The IoU scores of VACC versus ConceptFusion and LeRF.

world 3d scene understanding from 2d vision-language models, 2022. 2

[11] Yining Hong, Haoyu Zhen, Peihao Chen, Shuhong Zheng, Yilun Du, Zhenfang Chen, and Chuang Gan. 3d-llm: Injecting the 3d world into large language models, 2023. 1, 2

[12] Yafei Hu, Quanting Xie, Vidhi Jain, Jonathan Francis, Jay Patrikar, Nikhil Keetha, Seungchan Kim, Yaqi Xie, Tianyi Zhang, Shibo Zhao, Yu Quan Chong, Chen Wang, Katia Sycara, Matthew Johnson-Roberson, Dhruv Batra, Xiaolong Wang, Sebastian Scherer, Zsolt Kira, Fei Xia, and Yonatan Bisk. Toward general-purpose robots via foundation models: A survey and meta-analysis, 2023. 1

[13] Yihan Hu, Jiazhui Yang, Li Chen, Keyu Li, Chonghao Sima, Xizhou Zhu, Siqi Chai, Senyao Du, Tianwei Lin, Wenhai Wang, Lewei Lu, Xiaosong Jia, Qiang Liu, Jifeng Dai, Yu Qiao, and Hongyang Li. Planning-oriented autonomous driving, 2023. 1

[14] Chen Huang, Oier Mees, Andy Zeng, and Wolfram Burgard. Visual language maps for robot navigation. *2023 IEEE International Conference on Robotics and Automation (ICRA)*, pages 10608–10615, 2022. 2

[15] Krishna Murthy Jatavallabhula, Alihusein Kuwajerwala, Qiao Gu, Mohd Osama, Tao Chen, Alaa Maalouf, Shuang Li, Ganesh Iyer, Soroush Saryazdi, Nikhil Keetha, et al. Conceptfusion: Open-set multimodal 3d mapping. *arXiv preprint arXiv:2302.07241*, 2023. 1, 2, 3

[16] Chao Jia, Yinfai Yang, Ye Xia, Yi-Ting Chen, Zarana Parekh, Hieu Pham, Quoc V. Le, Yunhsuan Sung, Zhen Li, and Tom Duerig. Scaling up visual and vision-language representation learning with noisy text supervision, 2021. 2

[17] Xiaosong Jia, Liting Sun, Hang Zhao, Masayoshi Tomizuka, and Wei Zhan. Multi-agent trajectory prediction by combining egocentric and allocentric views. In *5th Annual Conference on Robot Learning*, 2021. 2

[18] Justin Kerr, Chung Min Kim, Ken Goldberg, Angjoo Kanazawa, and Matthew Tancik. Lrf: Language embedded radiance fields. *2023 IEEE/CVF International Conference on Computer Vision (ICCV)*, pages 19672–19682, 2023. 2, 3

[19] Alexander Kirillov, Eric Mintun, Nikhila Ravi, and Hanzi Mao et. al. Segment anything, 2023. 2

[20] Boyi Li, Kilian Q. Weinberger, Serge Belongie, Vladlen Koltun, and René Ranftl. Language-driven semantic segmentation, 2022. 2

[21] Feng Li, Hao Zhang, Huaizhe xu, Shilong Liu, Lei Zhang, Lionel M. Ni, and Heung-Yeung Shum. Mask dino: Towards a unified transformer-based framework for object detection and segmentation, 2022. 2

[22] Junnan Li, Dongxu Li, Silvio Savarese, and Steven Hoi. Blip-2: Bootstrapping language-image pre-training with frozen image encoders and large language models, 2023. 2

[23] Zhiqi Li, Wenhai Wang, Enze Xie, Zhiding Yu, Anima Anandkumar, Jose M. Alvarez, Ping Luo, and Tong Lu. Panoptic segformer: Delving deeper into panoptic segmentation with transformers, 2022. 2

[24] Guibiao Liao, Kaichen Zhou, Zhenyu Bao, Kanglin Liu, and Qing Li. Ov-nerf: Open-vocabulary neural radiance fields with vision and language foundation models for 3d semantic understanding. *ArXiv*, abs/2402.04648, 2024. 2

[25] Kunhao Liu, Fangneng Zhan, Jiahui Zhang, Muyu Xu, Yingchen Yu, Abdulmotaleb El-Saddik, Christian Theobalt, Eric P. Xing, and Shijian Lu. 3d open-vocabulary segmentation with foundation models. *ArXiv*, abs/2305.14093, 2023. 2

[26] Zhao Mandi, Shreeya Jain, and Shuran Song. Roco: Dialectic multi-robot collaboration with large language models, 2023. 1, 3

[27] Kirill Mazur, Edgar Sucar, and Andrew J. Davison. Feature-realistic neural fusion for real-time, open set scene understanding, 2022. 2

[28] Ben Mildenhall, Pratul P. Srinivasan, Matthew Tancik, Jonathan T. Barron, Ravi Ramamoorthi, and Ren Ng. Nerf: Representing scenes as neural radiance fields for view synthesis, 2020. 2

[29] OpenAI, Josh Achiam, Steven Adler, Sandhini Agarwal, Lama Ahmad, and Ilge Akkaya et. al. Gpt-4 technical report, 2024. [2](#)

[30] Songyou Peng, Kyle Genova, Chiyu "Max" Jiang, Andrea Tagliasacchi, Marc Pollefeys, and Thomas Funkhouser. Openscene: 3d scene understanding with open vocabularies, 2023. [2](#)

[31] Minghan Qin, Wanhua Li, Jiawei Zhou, Haoqian Wang, and Hanspeter Pfister. Langsplat: 3d language gaussian splatting, 2024. [2](#)

[32] Alec Radford, Jong Wook Kim, and Chris Hallacy et. al. Learning transferable visual models from natural language supervision, 2021. [2](#)

[33] Nur Muhammad (Mahi) Shafiuallah, Chris Paxton, Lerrel Pinto, Soumith Chintala, and Arthur Szlam. Clip-fields: Weakly supervised semantic fields for robotic memory. *ArXiv*, abs/2210.05663, 2022. [2](#)

[34] Edgar Sucar, Shikun Liu, Joseph Ortiz, and Andrew J. Davison. imap: Implicit mapping and positioning in real-time, 2021. [2](#)

[35] Takafumi Taketomi, Hideaki Uchiyama, and Sei Ikeda. Visual slam algorithms: A survey from 2010 to 2016. *IPSJ transactions on computer vision and applications*, 9:1–11, 2017. [2](#)

[36] Gemini Team, Rohan Anil, Sebastian Borgeaud, Yonghui Wu, Jean-Baptiste Alayrac, Jiahui Yu, Radu Soricut, Johan Schalkwyk, Andrew M Dai, Anja Hauth, et al. Gemini: a family of highly capable multimodal models. *arXiv preprint arXiv:2312.11805*, 2023. [2](#)

[37] Vadim Tschernezki, Iro Laina, Diane Larlus, and Andrea Vedaldi. Neural feature fusion fields: 3d distillation of self-supervised 2d image representations. *2022 International Conference on 3D Vision (3DV)*, pages 443–453, 2022. [2](#)

[38] Ashish Vaswani, Noam Shazeer, Niki Parmar, Jakob Uszkoreit, Llion Jones, Aidan N. Gomez, Łukasz Kaiser, and Illia Polosukhin. Attention is all you need, 2023. [1](#)

[39] Wenhao Yu, Nimrod Gileadi, Chuyuan Fu, Sean Kirmani, Kuang-Huei Lee, Montse Gonzalez Arenas, Hao-Tien Lewis Chiang, Tom Erez, Leonard Hasenclever, Jan Humplík, Brian Ichter, Ted Xiao, Peng Xu, Andy Zeng, Tingnan Zhang, Nicolas Heess, Dorsa Sadigh, Jie Tan, Yuval Tassa, and Fei Xia. Language to rewards for robotic skill synthesis, 2023. [1](#)

[40] Xizhou Zhu, Weijie Su, Lewei Lu, Bin Li, Xiaogang Wang, and Jifeng Dai. Deformable detr: Deformable transformers for end-to-end object detection, 2021. [2](#)

[41] Brianna Zitkovich, Tianhe Yu, Sichun Xu, Peng Xu, Ted Xiao, Fei Xia, Jialin Wu, Paul Wohlhart, Stefan Welker, Ayzaan Wahid, et al. Rt-2: Vision-language-action models transfer web knowledge to robotic control. In *Conference on Robot Learning*, pages 2165–2183. PMLR, 2023. [1](#)

[42] Arkaitz Zubiaga. Natural language processing in the era of large language models. *Frontiers in Artificial Intelligence*, 6, 2024. [1](#)